



# DYNAMIC ANALYSIS OF A STEEL-CONCRETE RAILWAY BRIDGES OF LANGER TYPE UNDER THE INFLUENCE OF A MOVING LOAD

## ANALIZA DYNAMICZNA STALOWO-BETONOWEGO MOSTU KOLEJOWEGO TYPU LANGERA POD WPŁYWEM OBCIĄŻENIA RUCHOMEGO

Waldemar Szaniec\*, Urszula Radoń  
Kielce University of Technology, Poland  
Adrián Bekő  
Slovak University of Technology, Slovakia

### Abstract

*The studying the dynamic response of steel-concrete railway bridges of Langer type is huge importance of ensuring the safety of such structures under high-speed train loads. Numerical simulations at the design stage require knowledge of the modal characteristics: natural frequencies, shapes and damping. In addition, in the dynamics of railway bridges subjected to high-speed trains, it is important to check the impact of dynamic effects on the ultimate and serviceability limit states. As part of the investigations displacements and accelerations of selected measurement points arising from driving the test rolling stock are analyzed. In the first stage, calculations of the eigenvalues and the corresponding eigenvectors were carried out in the Robot program for two variants of mass description (distributed and discrete). In the second stage, dynamic train passages for various vehicle speeds were examined in terms of displacements and accelerations of measurement points by using the authors' program MES3D.*

**Keywords:** modal analysis, Newmark method, FEM model, moving load, steel-concrete railway bridges of Langer type

### Streszczenie

*Badanie odpowiedzi dynamicznej stalowo-betonowych mostów kolejowych typu Langer ma ogromne znaczenie dla zapewnienia bezpieczeństwa takich obiektów pod obciążeniem pociągów dużych prędkości. Symulacje numeryczne na etapie projektowania wymagają znajomości charakterystyk modalnych: częstotliwości drgań własnych, form i tłumienia. Dodatkowo w dynamice mostów kolejowych poddanych działaniu pociągów szybkojeźdźnych istotne jest sprawdzenie wpływu efektów dynamicznych na stany graniczne nośności i użyteczności. W ramach badań analizowano przemieszczenia i przyspieszenia wybranych punktów pomiarowych powstałych od jazdy taborem próbnym. W pierwszym etapie przeprowadzono obliczenia wartości własnych i odpowiadających im wektorów własnych w programie Robot dla dwóch wariantów opisu masy (rozłożonej i dyskretniej). W drugim etapie zbadano przebiegi dynamiczne dla różnych prędkości pociągów pod kątem przemieszczeń i przyspieszeń punktów pomiarowych za pomocą autorskiego programu MES3D.*

**Słowa kluczowe:** analiza modalna, metoda Newmarka, model MES, obciążenie ruchome, stalowo-betonowe mosty kolejowe typu Langer

\*Kielce University of Technology, Poland, e-mail: [wszaniec@tu.kielce.pl](mailto:wszaniec@tu.kielce.pl)

## 1. INTRODUCTION

Nowadays, transport needs are still increasing. Bridges ensure a collision-free intersection of pedestrian routes with roads, railways and waterways. These structures are often characterized by interesting architectural forms. This is mainly due to the use of modern high-strength materials and the increase in the possibilities and accuracy of design calculations, e.g. using the finite element method (FEM) in the design process. Numerical calculations are often verified by in-situ experimental studies [1-8]. The numerical simulations of dynamic behavior at the design stage require knowledge of the modal characteristics of the structural system. These are sets of natural frequencies, mode shapes, and damping. There are two general methods for determining the modal characteristics of structures: analytical and experimental. The first one usually employs a modal analysis performed on a numerical model [9-15], which can be done at the design stage but has limitations resulting from simplifying assumptions, mainly concerning damping, joint stiffness, and boundary conditions. On the other hand, the experimental method comprises conducting a field test to determine the modal characteristics of the real structure. For identification, controlled experiments are performed [16] and most often analyzed by experimental modal analysis (EMA) [17, 18] or operational modal analysis (OMA) [18, 19].

In addition, in the dynamics of railway bridges subjected to high-speed trains, it is important to check the impact of dynamic effects on the ultimate and serviceability limit states. Serviceability limit states are related to driving safety and passenger comfort. An increase in the operating speed results in increased actions by railway vehicles on the structure and entails the need to solve numerous complex engineering problems. From the perspective of traffic safety and travel comfort (particularly relevant in case of high operating speeds) it is important to determine vibration amplitudes for both the vehicle and bridge spans and the interacting forces between them. Numerical simulations of bridge load tests are often performed before they are put into service. Their purpose is to verify the actual condition of the structure and correlation of measurement results with theory. This enables, among others, commissioning objects without the need to carry out costly measurements of vehicles acting on the structure other than those for which designated tests are required. Currently structural analyses are performed mainly using finite element computer programs. They provide a very

accurate representation of a structure with beam, shell and solid elements. The modelling method is chosen depending on the objective of the analysis. Technical problems related to the description of the dynamic response of railway bridges are discussed in [20-27].

From the point of view of bridge structures, the moving load is one of the most important components of the load. The analysis of the impact of the moving load on bridge structures is carried out numerically or experimentally. The numerical approach requires attention to the following issues: creating computational models of the vehicle and bridge, creating computational programs to solve equations of motion. To solve this problem, it is beneficial to work with discrete computational models using the finite element method. The experimental approach focuses on verifying the adopted numerical models and monitoring the condition of bridge structures. One of the key elements of structural health monitoring (SHM) is operational modal analysis. Identification of the modal properties of a structural system is a process of correlating the dynamic characteristics of a numerical model with the physical properties of the system obtained from experimental measurements. This allows engineers to analyze structural behavior and identify potential structural failures.

Polish State Railways's (PKP) development plans include the introduction of express passenger trains moving at speeds of up to 250 km/h on the Central Railway Main Line (CMK). One of the scientific and technical problems related to this is to check the dynamic strain of bridge structures on CMK in new operating conditions. The basic group of these objects are composite beam bridges with a load-bearing structure consisting of steel plate girder main beams and a reinforced concrete bridge slab. The presented work concerns the numerical analysis of the bridge structure along the PKP line No. 4 CMK on the section Szeligi - Idzikowice at km 26.571/26.578 under dynamic load. The subject of the research is the supporting structure of the viaduct. It is a steel Langer arch (rigid deck and slender arch) located over the S8 expressway (Figs. 1, 2). In the first stage, calculations of the eigenvalues and the corresponding eigenvectors were carried out. The modal analysis of the bridge was performed for a spatial FEM model. The calculations were carried out in the Robot program for two variants of mass description (distributed and discrete). In the second stage, dynamic passages for various train speeds were examined in terms of displacements and accelerations of measurement points. Two variants of the load were

adopted in the work. The first consists of ES64U4 electric locomotive located at the beginning and end of the train and four 154A type passenger cars (Fig. 3a). In the first variant the load moves at the following speeds: 10, 40, 80, 120, 160, 180 and 200 km/h. Due to the symmetry of the structure and the measuring points, the load motion was simulated in one direction. The second variant consists of the ETR610 Pendolino located at the beginning and end of the train and five passenger cars (Fig. 3b). The following velocities were assumed: 10, 200, 230 and 250 km/h. Seven recording points were defined on the structural model. In three locations on one side vertical displacements, horizontal displacements in two perpendicular directions and vertical accelerations were recorded, while in all other points only vertical displacements were tracked. The

calculations were carried out using the proprietary MES3D program developed by the authors.

In summary, the manuscript focuses on two themes. At first, the analytical identification of the bridge modal response is sought (eigenfrequencies are determined in two variants of mass representation: concentrated and distributed) to enable and improve further numerical computations. Secondly, the structural response is predicted, in terms of displacements and accelerations, for various vehicle speeds of two train load sets. Finally, conclusions are formulated on the basis of the obtained data to address the serviceability of the object and human voyage comfort. The studying the dynamic response of steel-concrete railway bridges of Langer type is huge importance of ensuring the structural integrity and safety of such bridges under high-speed train loads.



Fig. 1. Side view of the bridge (<https://www.google.com/maps>)



Fig. 2. Bottom view of the bridge (<https://www.google.com/maps>)

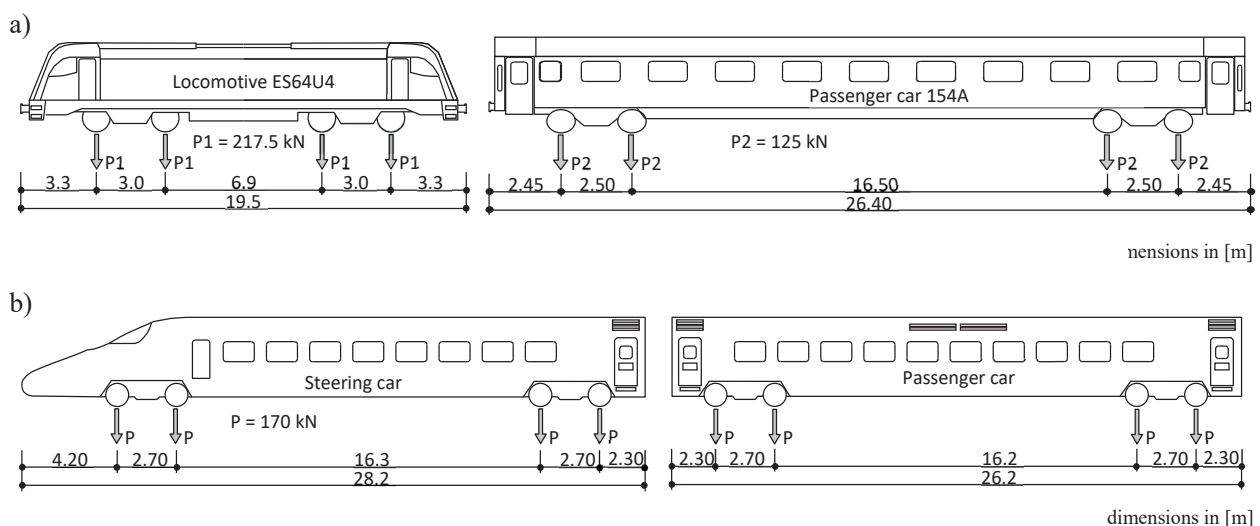


Fig. 3. Two variants of moving load: a) ES64U4 electric locomotive located at the beginning and end of the train and four 154A type passenger cars, b) ETR610 Pendolino located at the beginning and end of the train and five passenger cars

## 2. MATERIAL AND METHODS

### 2.1. Modal analysis

One of the basic issues in dynamics of structures is to determine the conditions under which the system can move around the equilibrium position without the action of external forcing forces. The matrix differential equation of motion describing this process without damping can be written as:

$$\mathbf{M}\ddot{\mathbf{q}} + \mathbf{K}\mathbf{q} = \mathbf{0} \quad (1)$$

where:

$\mathbf{M}$  – mass matrix,

$\mathbf{K}$  – stiffness matrix,

$\mathbf{q}$  – vector of nodal displacements,

$\omega$  – eigenfrequency.

Predicting a harmonic solution, suppose:

$$\ddot{\mathbf{q}} = -\omega^2 \mathbf{q} \quad (2)$$

Substituting expression (2) into equation (1) we obtain a homogeneous matrix equation that must be satisfied at any arbitrary time  $t$ .

$$(\mathbf{K} - \omega^2 \mathbf{M}) = \mathbf{0} \quad (3)$$

The trivial solution does not yield the searched conditions of the problem as it corresponds to equilibrium at rest. The condition for the existence of non-zero solutions is the equation:

$$\det|\mathbf{K} - \omega^2 \mathbf{M}| = 0 \quad (4)$$

After solving the determinant, we obtain an algebraic equation with respect to  $\omega$  whose roots are the eigenfrequencies of the structure. These roots are real positive numbers, and their number is equal to the number of dynamic degrees of freedom (multiple roots may be present). Each eigenvalue  $\omega_i$  corresponds to a solution  $\mathbf{q} = \mathbf{w}_i$  such that:

$$(\mathbf{K} - \omega_i^2 \mathbf{M})\mathbf{w}_i = \mathbf{0} \quad (5)$$

The vector  $\mathbf{w}_i$  is called the eigenvector of the  $i$ -th mode of vibration. It determines the distribution of displacements during vibrations with the frequency  $\omega_i$ . Eigenvectors are defined up to a constant factor, so they can be normalized arbitrarily. The set of eigenvectors forms an eigenmatrix  $\mathbf{W}$ .

$$\mathbf{W} = [\mathbf{w}_1, \mathbf{w}_2, \dots, \mathbf{w}_d] \quad (6)$$

where  $d$  is the number of dynamic degrees of freedom.

Modal analysis allows us to effectively solve structural problems related to vibration at the design or operation stage. Its main application is to compare the frequency of excitation of the system with its natural frequencies. If these values are close to each other or overlap, the phenomenon of resonance arises. During resonance, vibration amplitudes can be multiplied multiple times, which may lead to failure or complete destruction of the structure.

### 2.2. Newmark method (average acceleration)

Newmark implicit time integration method is one of the oldest and most powerful methods used for dynamic analysis of structures and wave propagation problems. Newmark's method, [28], allows the direct solution of a second-order differential equation or a system of second-order differential equations. Consider the matrix equation of motion:

$$\mathbf{M}\ddot{\mathbf{q}} + \mathbf{C}\dot{\mathbf{q}} + \mathbf{K}\mathbf{q} = \mathbf{P} \quad (7)$$

with initial conditions:

$$\mathbf{q}(0) = \mathbf{q}_0 \quad (8)$$

$$\dot{\mathbf{q}}(0) = \dot{\mathbf{q}}_0 \quad (9)$$

where:

$\mathbf{M}$  – mass matrix,

$\mathbf{K}$  – stiffness matrix,

$\mathbf{C}$  – damping matrix,

$\mathbf{q}$  – vector of nodal displacements,

$\mathbf{P}$  – vector of nodal load.

Vector  $\mathbf{P}$  for  $t \geq 0$  contains components that are arbitrary, continuous functions of time. The equation in the general case is a description of some non-stationary dynamic process. Analytical solution of the equation of motion for arbitrary forces may prove difficult, hence direct methods of numerical integration are of great practical importance. If we choose a discrete set of points  $t_i$  on the time axis with the integration step  $h = t_{i+1} - t_i$ , then the representation of the solution of the equation will be the set of vectors displacements and velocities. The calculations use the Newmark method, which can be formulated by expanding the function into a Taylor series

$$\dot{\mathbf{q}}_{i+1} = \dot{\mathbf{q}}_i + h\ddot{\mathbf{q}}_i + \frac{1}{2}h^2\dddot{\mathbf{q}}_i + \dots \quad (10)$$

$$\mathbf{q}_{i+1} = \mathbf{q}_i + h\dot{\mathbf{q}}_i + \frac{1}{2}h^2\ddot{\mathbf{q}}_i + \frac{1}{6}h^3\dddot{\mathbf{q}}_i + \dots \quad (11)$$

Higher derivatives are eliminated from the formulas (12) and (13), leaving terms of the second order at most. We replace the remaining terms of the Taylor expansion with arithmetic means for velocities and weighted averages for displacements.

$$\dot{\mathbf{q}}_{i+1} = \dot{\mathbf{q}}_i + \frac{1}{2}h\ddot{\mathbf{q}}_i + \frac{1}{2}h\ddot{\mathbf{q}}_{i+1} \quad (12)$$

$$\mathbf{q}_{i+1} = \mathbf{q}_i + h\dot{\mathbf{q}}_i + \left(\frac{1}{2} - \beta\right)h^2\ddot{\mathbf{q}}_i + \beta h^2\ddot{\mathbf{q}}_{i+1} \quad (13)$$

where: parameter  $\beta \in (0; \frac{1}{2})$ .

From the last relationship, we get:

$$\ddot{\mathbf{q}}_{i+1} = \frac{1}{\beta h^2} \left[ \mathbf{q}_{i+1} - \mathbf{q}_i - h\dot{\mathbf{q}}_i - \left(\frac{1}{2} - \beta\right)h^2\ddot{\mathbf{q}}_i \right] \quad (14)$$

In the Newmark method as an interpolation method, the collocation condition is satisfied at the time 'i+1'.

$$\mathbf{M}\ddot{\mathbf{q}}_{i+1} + \mathbf{C}\dot{\mathbf{q}}_{i+1} + \mathbf{K}\mathbf{q}_{i+1} = \mathbf{P}_{i+1} \quad (15a)$$

$$\begin{aligned} & \frac{1}{\beta h^2} \mathbf{M} \left[ \mathbf{q}_{i+1} - \mathbf{q}_i - h\dot{\mathbf{q}}_i - \left(\frac{1}{2} - \beta\right)h^2\ddot{\mathbf{q}}_i \right] + \\ & + \mathbf{C} \left[ \dot{\mathbf{q}}_i + \frac{1}{2}h\ddot{\mathbf{q}}_i + \frac{1}{2}h\frac{1}{\beta h^2} \left[ \mathbf{q}_{i+1} - \mathbf{q}_i - h\dot{\mathbf{q}}_i - \right. \right. \\ & \left. \left. - \left(\frac{1}{2} - \beta\right)h^2\ddot{\mathbf{q}}_i \right] \right] + \mathbf{K}\mathbf{q}_{i+1} = \mathbf{P}_{i+1} \end{aligned} \quad (15b)$$

After tidying up, we can write:

$$\mathbf{A} \cdot \mathbf{q}_{i+1} = \mathbf{R}_{i+1} \quad (16)$$

where:

$$\begin{aligned} \mathbf{A} &= \frac{1}{\beta h^2} \mathbf{M} + \frac{1}{2\beta h} \mathbf{C} + \mathbf{K} \\ \mathbf{R}_{i+1} &= \mathbf{P}_{i+1} + \left[ \frac{1}{\beta h^2} \mathbf{q}_i + \frac{1}{\beta h} \dot{\mathbf{q}}_i + \left(\frac{1}{2\beta} - 1\right) \ddot{\mathbf{q}}_i \right] \mathbf{M} + \\ & + \left[ \frac{1}{2\beta h} \mathbf{q}_i - \left(\frac{1}{2\beta} - 1\right) \dot{\mathbf{q}}_i + \frac{h}{2} \left(\frac{1}{2\beta} - 2\right) \ddot{\mathbf{q}}_i \right] \mathbf{C} \end{aligned}$$

When initiating the solution process, the vector  $\ddot{\mathbf{q}}_0$  is needed to determine the modified vector  $\mathbf{R}_1$ . It can be calculated by writing the collocation equation for time  $t = 0$  as

$$\ddot{\mathbf{q}}_0 = \mathbf{M}^{-1} (\mathbf{P}_0 - \mathbf{C}\dot{\mathbf{q}}_0 - \mathbf{K}\mathbf{q}_0) \quad (17)$$

The numerical solution is always burdened with an error resulting from the use of a finite step size, the so-

called discretization error. In addition, there may be effects of the so-called parasitic damping, which result from the very formulation of the method. In the case of the Newmark method, the stability of the scheme is determined by the value of the  $\beta$  parameter. For  $0.25 \leq \beta \leq 0.5$  the scheme is unconditionally stable. For the range  $0 \leq \beta < 0.25$  the scheme is conditionally stable with a stability limit.

$$h < \frac{2}{\omega \sqrt{1 - 4\beta}} \quad (18)$$

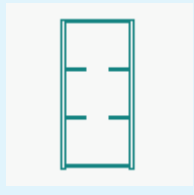
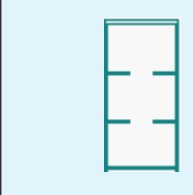
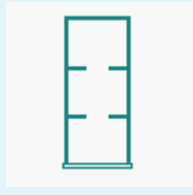
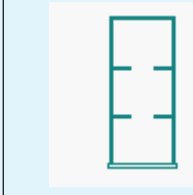
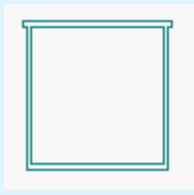
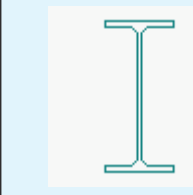
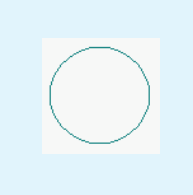
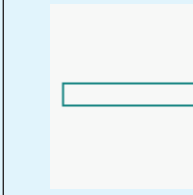
In our calculations, an unconditionally stable variant with a beta parameter of 0.25 was used. For the practical application of stability conditions, it is necessary to know the highest natural frequency of the analyzed structure. This requirement greatly limits the possibilities for calculating the limiting time step. In addition to stability, the accuracy of the solution should also be considered. Unfortunately, the higher the stability, the lower the accuracy.

### 3. EXAMPLE - DESCRIPTION, CALCULATIONS, RESULTS AND DISCUSSION

#### 3.1. Description of steel-concrete railway bridge of Langer type

The supporting structure of the viaduct is a steel Langer arch with rigid deck and slender arch (Fig. 4). Technical parameters of the viaduct: theoretical length 75 m, construction height 1.59 m, crossbar spacing 2.5 m, main girder spacing 5 m, hangers spacing 7.5 m. The platform was built of a steel plate girder and an orthotropic slab. Steel fixed and movable double-roller bearings provide support for the spans. For each track there are separate supports of the viaduct, which are offset from each other because the road under the viaduct is laid diagonally. Franc piles support the massive abutments of the second geotechnical category and retaining walls. The structure is equipped with a railway superstructure made of UIC60 rails with SB type fastening on reinforced concrete sleepers, where rail profiles are placed. The cross-section of the arch is a steel box with a height of 1534 mm and a width of 730 mm. These dimensions are constant along its entire length, but the thickness of the sheet varies: at the beginning and end of the arch it is 28 mm, while in the middle it is 24 mm (Table 1). The bottom chord is built in a similar way, it is also a steel box with a constant cross-section along the entire length: 1792 mm high and 730 mm wide and of different sheet thickness: 28 mm at the two ends of the structure and 20 mm in

Table 1. Sections of the supporting structure of the viaduct

Section				
Description	Upper chord – external elements	Upper chord – middle elements	Bottom chord – external element	Bottom chord – middle elements
A [cm <sup>2</sup> ]	1494.24	1377.28	1660.15	1385.12
I <sub>x</sub> [cm <sup>4</sup> ]	2839631.79	2555241.10	3769659.90	2952872.06
I <sub>y</sub> [cm <sup>4</sup> ]	4374418.85	4165103.38	6643890.18	5966576.30
I <sub>z</sub> [cm <sup>4</sup> ]	1235736.37	1115075.81	15317361.91	1218094.99
Section				
Description	Crossbeam – upper chord	Crossbeam of the deck slab	Hanger	Sling
A [cm <sup>2</sup> ]	560.40	306.00	50.27	350.00
I <sub>x</sub> [cm <sup>4</sup> ]	470254.32	833.00	398.78	5269.89
I <sub>y</sub> [cm <sup>4</sup> ]	423258.02	256900.00	201.06	1429.17
I <sub>z</sub> [cm <sup>4</sup> ]	278602.03	14440.00	201.06	72916.67

the middle. The load-bearing structure of the deck slab is made of the HEB profile. These elements have been moved to their actual position using offsets. The arched upper chord is connected with rectangular box section cross-beams. The structure was modeled in the Autodesk Robot program as a spatial structure. Bar elements were used to model the steel parts. The reinforced concrete slab with a thickness of 30 cm, on which the track is located, was modeled using shell elements without reinforcement. The computational model contained 548 nodes, 168 bar elements and 120 shell elements. The total number of generalized coordinates is 3288. The dynamic analysis took into account the mass of equipment elements located on the bridge: brackets, balustrades, track elements. The value per one girder was equal to 1950 kg/m, added to the longitudinal members of the bottom chord.

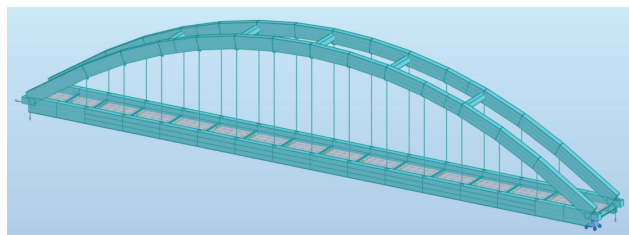


Fig. 4. FEM model of the steel-concrete railway bridge of the Langer type

### 3.2. Modal analysis of railway bridge of Langer type

The modal analysis was performed in the Robot program with continuous and discrete mass field distributions. In engineering practice, we are most often interested in the lowest vibration frequencies. In the variant with continuous mass distribution we also obtain vibration modes related to the movement of individual structural elements, e.g. hangers (Fig. 5), which might not be of interest to us. Hangers, which are fragment of structure in case continuous mass distribution can give independent forms of vibration. However, their influence on the vibration of the entire structure is small. Such vibration modes usually do not occur with discrete mass distribution. Independent forms of hanger vibrations are directly related to the way they are installed in the structure. The hangers are hinged to the gusset plate. Slight differences between the vibration frequencies result from the ways of describing the mass distribution for both models in FEM (Table 2). The comparison of the first six vibration frequencies for the model with concentrated masses and with the distributed mass model is shown in Table 2. Further calculations and illustrations of the vibration mode shapes are given for the to the discrete mass model (Fig. 6).

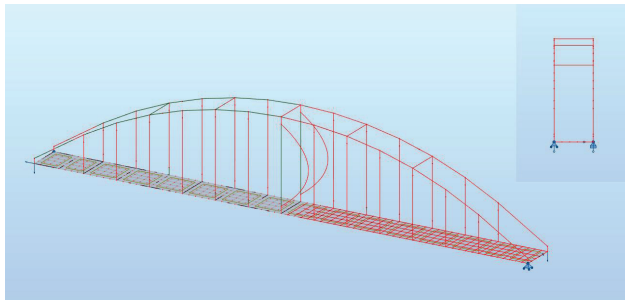


Fig. 5. Vibration mode shape related to the local movement of an individual hanger

Table 2. The comparison of the first six vibration frequencies for the model with concentrated masses and with the distributed mass model

Nr form	Frequency [Hz]	
	Discrete mass	Distributed mass
1	1.09	1.10
2	2.14	2.15
3	2.44	2.48
4	3.19	3.21
5	3.69	3.68
6	4.77	4.84

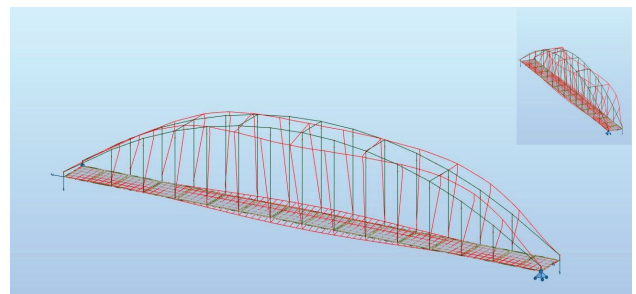
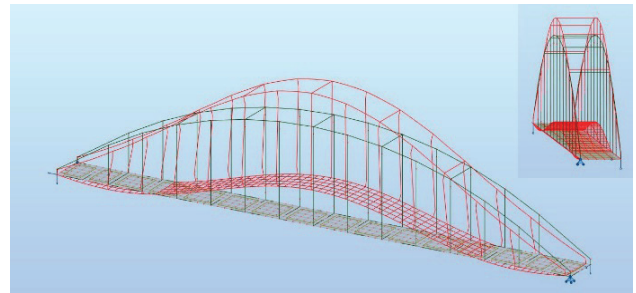
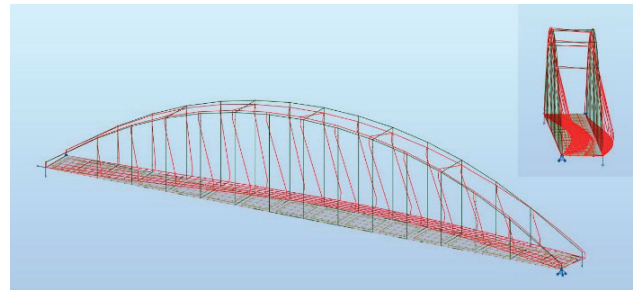
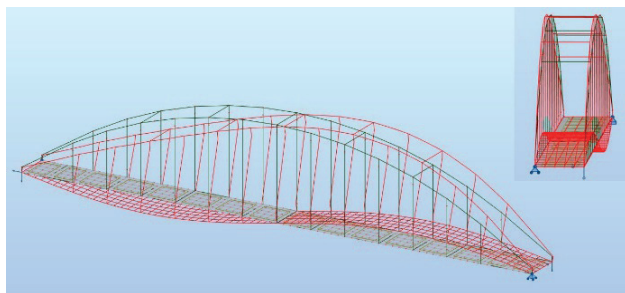
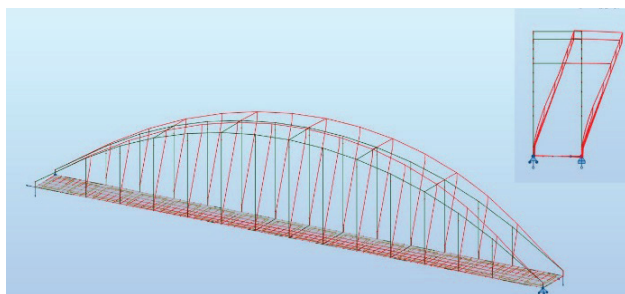


Fig. 6. First six mode shapes of numerical model with discrete mass distribution

### 3.3. Calculations of railway bridge under the influence of the moving load

The calculations under the influence of the moving load were made in the MES3D program using the unconditionally stable variant of the Newmark method [28]. Experience shows that in the case of engineering analyzes of real objects, it is sufficient to assume that the load operates in a non-inertial manner, the time of computer simulations is significantly shorter in such case.

The calculations did not directly take into account the elastic characteristics of the subgrade (track, ballast), the fact of indirect load transfer to the structure was taken into account by adopting a load model in which the pressure of a single concentrated force  $N$  is replaced by three forces at intervals of 0.5 m and weighting factors  $N/4$ ,  $N/2$ ,  $N/4$ . The forward motion of the load was assumed in steps of  $\Delta x = 0.02$  m. Based on this the size of the time step was determined as  $h = \Delta t = \Delta x/v$ . The layout of the pick-up points is shown in Figure 7.

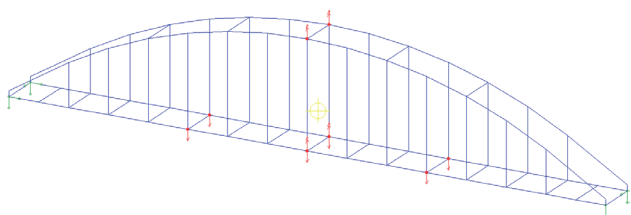


Fig. 7. Location of recording points

Tables 3 and 4 show the maximum values of deflections and accelerations of points obtained for the considered travel speeds of the ES64U4 and Pendolino trains. On this basis, the values of dynamic coefficients were determined for the tested quantities. Figures 8-17 shows the dynamic response of selected points – vertical deflections of points at one quarter

and one half of the span under the right girder and vertical accelerations at the upper and lower end of the hanger in the middle of the span.

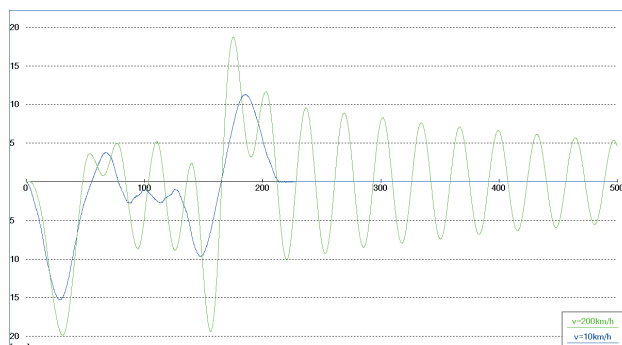


Fig. 8. Dynamic runs of the vertical displacement of the UzP3 point at the speed of 10 and 200 km/h for the ES64U4 train

Table 3. Displacements and accelerations of selected points for different speeds of the ES64U4 train

Velocity [km/h]	Displacements [mm]						Accelerations [m/s <sup>2</sup> ]			
	UzP3	UzP7	UzP11	UzL3	UzL7	UzL11	PzP7D	PzP7G	PzL7D	PzL7G
static	15.27	9.15	15.21	15.27	9.17	15.21	–	–	–	–
10	15.28	9.16	15.27	15.28	9.16	15.27	0.01	0.03	0.01	0.03
40	15.26	9.26	16.24	15.26	9.28	16.3	0.08	0.15	0.07	0.15
80	15.36	9.31	16.17	15.34	9.25	16.22	0.06	0.06	0.06	0.07
120	16.14	9.38	17.31	16.14	9.42	17.34	0.15	0.13	0.17	0.14
160	17.41	9.70	19.92	17.39	9.56	20.07	0.28	0.28	0.25	0.26
180	21.00	9.60	25.30	20.86	9.78	25.47	0.26	0.27	0.27	0.31
200	19.89	10.00	21.19	19.87	9.96	21.44	0.32	0.33	0.33	0.35
dynamic coefficient	1.38	1.09	1.66	1.37	1.09	1.67	–	–	–	–

Table 4. Displacements and accelerations of selected points for different speeds of the ETR610 Pendolino train

Velocity [km/h]	Displacements [mm]						Accelerations [m/s <sup>2</sup> ]			
	UzP3	UzP7	UzP11	UzL3	UzL7	UzL11	PzP7D	PzP7G	PzL7D	PzL7G
static	10.51	5.95	10.51	10.51	5.95	10.51	–	–	–	–
10	10.51	5.95	10.51	10.5	5.95	10.51	0.01	0.06	0.02	0.05
200	11.15	6.92	11.61	11.18	7.02	11.73	0.48	0.53	0.5	0.55
230	10.29	7.18	10.20	10.28	7.17	10.21	0.54	0.6	0.52	0.6
250	11.21	10.15	10.83	11.18	10.12	10.87	1.49	1.54	1.5	1.54
dynamic coefficient	1.07	1.71	1.10	1.06	1.70	1.12	–	–	–	–



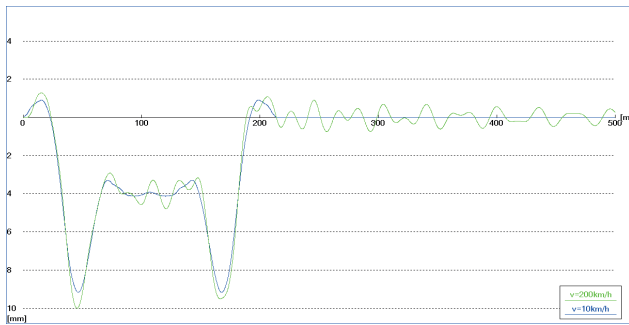


Fig. 9. Dynamic runs of the vertical displacement of the UzP7 point at the speed of 10 and 200 km/h for the ES64U4 train

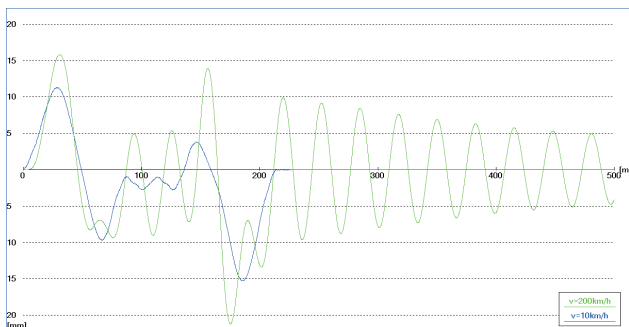


Fig. 10. Dynamic runs of the vertical displacement of the UzP11 point at the speed of 10 and 200 km/h for the ES64U4 train

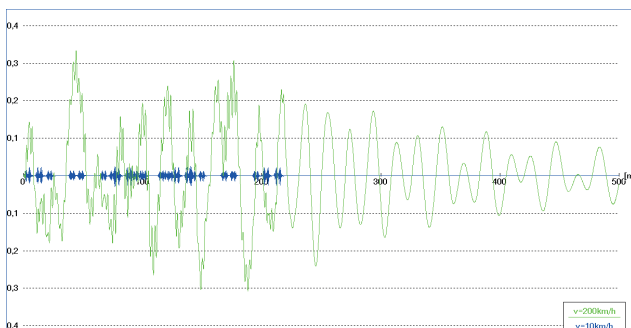


Fig. 11. Dynamic runs of the vertical acceleration of the PzP7G point at speeds of 10 and 200 km/h for the ES64U4 train

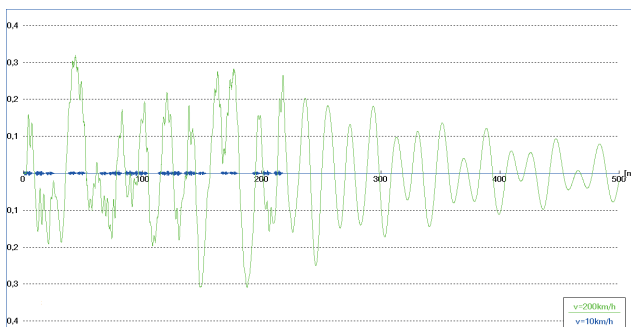


Fig. 12. Dynamic runs of the vertical acceleration of the PzP7D point at speeds of 10 and 200 km/h for the ES64U4 train

Analyzing the displacement diagrams for the ES64U4 train (Figs. 8-10), it can be seen that the

impact of dynamic load for the extreme points (UzP3, UzP11) is much greater than for the middle point (UzP7). After removing the load from the bridge, the extreme points perform free damped vibrations, for the middle point they are more complex. The acceleration diagrams of the upper and lower ends of the PzP7 hanger (Figs. 11, 12) have a similar shape and similar values. However, their nature is slightly different. In the upper belt there are definitely larger oscillations. This is related to the lower stiffness of the arch girder in relation to the stiffness of the deck.

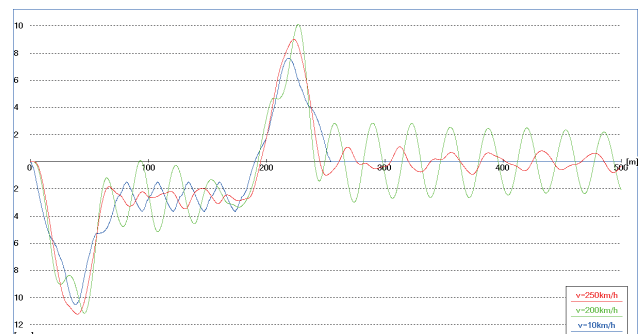


Fig. 13. Dynamic runs of the vertical displacement of the UzP3 point at speeds of 10, 200 and 250 km/h for the ETR610 Pendolino train

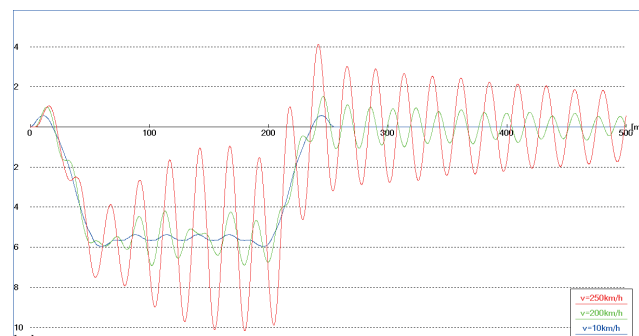


Fig. 14. Dynamic runs of the vertical displacement of the UzP7 point at speeds of 10, 200 and 250 km/h for the ETR610 Pendolino train

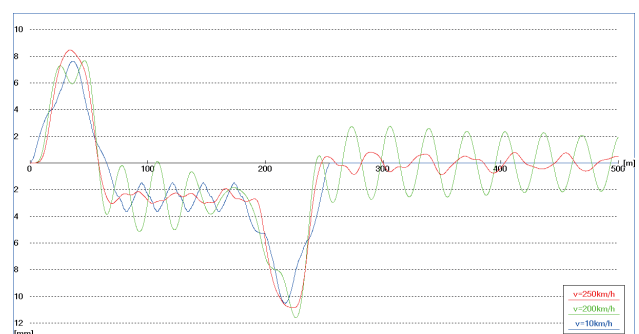


Fig. 15. Dynamic runs of the vertical displacement of the UzP11 point at speeds of 10, 200 and 250 km/h for the ETR610 Pendolino train

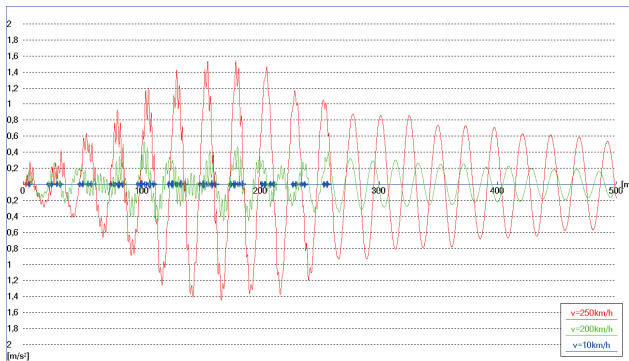


Fig. 16. Dynamic runs of vertical acceleration of the PzP7G point at speeds of 10, 200 and 250 km/h for the ETR610 Pendolino train

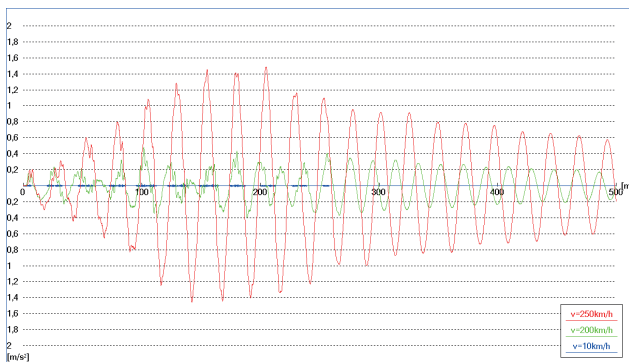


Fig. 17. Dynamic runs of vertical acceleration of the PzP7D point at speeds of 10, 200 and 250 km/h for the ETR610 Pendolino train

When traveling with the Pendolino train (Figs. 13-15), the displacements for the analyzed points are comparable to those of the ES64U4 train, except for the midpoint for the speed of 250 km/h, where we can observe much greater dynamic effects. For the Pendolino load for speeds of 10 and 200 km/h, the acceleration values (Figs. 16, 17) are similar to those for the ES64U4 train. A significant increase occurs at a speed of 250 km/h. However, the obtained acceleration values are acceptable both in terms of travel safety and travel comfort.

Comparing the ES64U4 and Pendolino trains, we can observe slightly different dynamic effects in the structure. This is related to the geometry of the bridge and the distribution of loading forces. In the case of the Pendolino train, the values of the forces are the same, in the ES64U4 train, the locomotive forces are about 1.74 times greater than those of the wagons. This results in greater changes in deflections, and consequently also vibrations, when the locomotive approaches or exits the structure. The obtained values of dynamic coefficients for individual measurement points (Tables 2 and 3) are characterized by high

variability, they range from 1.06 to 1.71. There is no proportional relationship between their value and the load speed. Even for the same measurement point (e.g. UzP7) for crossings of different types of trains, the dynamic coefficient reaches the values of 1.09 or 1.71.

#### 4. CONCLUSIONS

Railway infrastructure facilities are highly exposed to dynamic factors. With the development of computer tools, numerical simulations of such structures have become possible. Modal analysis is one of the simplest to perform, here it was carried out in the Autodesk Robot program for various variants of the mass distribution. In the case of the considered object, it was more convenient to use a discrete distribution, thus avoiding the inclusion of frequencies associated with local vibrations of individual elements, and not the structure as a whole. For both mass models, the basic vibration frequencies were similar. In the case of this type of objects, however, it can be difficult to assess the vibration mode shapes as it is not always possible to clearly determine whether it is a pure bending or torsional or other mode. The modes are usually clear only for the first couple of frequencies. In the case of the analyzed structure, the first natural frequency in an out-of-plane bending mode was equal to 1.1 Hz, and that of in-plane bending vibrations was 2.12 Hz. The first torsional mode was found at 2.44 Hz. Operational tests were carried out for this structure by the Road and Bridge Research Institute in Kielce. The results obtained were similar, which proves the correctness of the built model [29].

According to the PN-EN standards [30-35], the knowledge of the first frequencies of bending and torsional vibrations enables the decision to perform a dynamic analysis. This analysis was made using the MES3D program for two trainsets. The values of displacements and accelerations for the adopted measurement points were examined. The obtained maximum values of vertical accelerations do not exceed the value of  $1.6 \text{ m/s}^2$ , so they are within the range allowed by the standard, both in terms of travel comfort and traffic safety.

When designing the superstructure, we often use the standard dynamic coefficient. However, it has a global character and is not directly related to the velocity of the load nor does it always correctly reflect the behavior of individual parts of the structure. The values of dynamic coefficients obtained here for some measurement points are relatively high. Nonetheless, these coefficients are local and do not suggest a threat to the safe operation of the structure.

Analyzing the results presented in Tables 3 and 4, it appears that the dynamic effects do not always increase proportionally to the increase in speed.

It should also be clearly emphasized that the results of numerical calculations, especially dynamic ones, are

not always consistent with the results of tests carried out on real objects, discrepancies may result from errors and imperfections in modeling the structure and load, description of damping, etc., therefore they should be supported by operational tests.

## REFERENCES

- [1] Sokol M., Venglár M., Lamperová K., Márfoldi M.: *Performance Assessment of a Renovated Precast Concrete Bridge Using Static and Dynamic Tests*. Applied Sciences. Vol. 10. 2020. pp. 1-19.
- [2] Binczyk M., Żóltowski K.: *Launching of steel bridge girder. Application of nonlinear shell models*. CRC Press Taylor & Francis/Balkema, 2019.
- [3] Tomasik J., Obara P.: *Dynamic stability of tensegrity structures – Part 1: The time – independent external load*, Materials, 16(2), 580, 2023.
- [4] Radoń U., Zabojszcza P., Sokol M.: *The Influence of Dome Geometry on the Results of Modal and Buckling Analysis*, Applied Sciences – Basel, 13, 2729, 2023.
- [5] Lamperová K., Sokol M., Timková B.: *Identification of Bearings State on the Bridge Checked by Dynamic Tests*. Journal of Mechanical Engineering. Vol. 70. 2020. pp. 67-76.
- [6] Živanović S., Pavić A., Reynolds P.: *Finite element modelling and updating of a lively footbridge: The complete process*. J Sound Vib 2007;301(1-2):126-45. <http://dx.doi.org/10.1016/j.jsv.2006.09.024>.
- [7] Sokol M., Ároch R., Lamperová K., Marton M., García-Sanz-Caledo J.: *Parametric Analysis of Rotational Effects in Seismic Design of Tall Structures*. Applied Sciences. Vol 11. 2021. pp. 1-13.
- [8] Sokol M., Márfoldi M., Venglár M., Lamperová K.: *Evaluation of Performance Indicator of Railway Bridges Using Updated Finite Element Model*. Journal of Mechanical Engineering. 2019. Vol. 69. pp. 89-96.
- [9] Venglár M., Sokol M.: *Case study: The Harbor Bridge in Bratislava*. Structural Concrete. vol. 21. 2020. pp. 2736-2748.
- [10] Banas A., Jankowski R.: *Experimental and numerical study on dynamics of two footbridges with different shapes of girders*. Appl Sci 2020;10(13):4505.
- [11] Zhang L., Huang J.Y.: *Dynamic interaction analysis of the high-speed maglev vehicle/guideway system based on a field measurement and model updating method*. Eng Struct 2019;180(December 2017):1-17. <http://dx.doi.org/10.1016/j.engstruct.2018.11.031>.
- [12] Pradelok S., Jasiński M., Kocański T., Poprawa G.: *Numerical determination of dynamic response of the structure on the example of arch bridge*. Procedia Eng 2016;161:1084-9. <http://dx.doi.org/10.1016/j.proeng.2016.08.852>.
- [13] Caetano E., Cunha A., Magalhães F., Moutinho C.: *Studies for controlling human-induced vibration of the Pedro e Inês footbridge. Portugal*. Part 1: Assessment of dynamic behaviour. Eng Struct 2010;32(4):1069-81. <http://dx.doi.org/10.1016/j.engstruct.2009.12.034>.
- [14] Drygala I.J., Dulinska J.M.: *Full-scale experimental and numerical investigations on the modal parameters of a single-span steel-frame footbridge*. Symmetry 2019;11(3):404. <http://dx.doi.org/10.3390/sym11030404>.
- [15] Magalhães F., Cunha A., Caetano E., Brincker R.: *Damping estimation using free decays and ambient vibration tests*. Mech Syst Signal Process 2010;24(5):1274-90. <http://dx.doi.org/10.1016/j.ymssp.2009.02.011>.
- [16] Pavić A., Armitage T., Reynolds P., Wright J.: *Methodology for modal testing of the millennium bridge*. London. Proc Inst Civ Eng – Struct Build 2002;152(2):111-21. <http://dx.doi.org/10.1680/stbu.2002.152.2.111>.
- [17] Grebowski K., Rucka M., Wilde K.: *Non-destructive testing of a sport tribune under synchronized crowd-induced excitation using vibration analysis*. Materials 2019;12(13):2148. <http://dx.doi.org/10.3390/ma12132148>.
- [18] Brincker R., Ventura C.E.: *Introduction to operational modal analysis*. Chichester. West Sussex: Wiley; 2015. pp. 1-360. <http://dx.doi.org/10.1002/9781118535141>.
- [19] Brownjohn J.M.W., Magalhaes F., Caetano E., Cunha A.: *Ambient vibration retesting and operational modal analysis of the humber bridge*. Eng Struct 2010;32(8):2003-18. <http://dx.doi.org/10.1016/j.engstruct.2010.02.034>.
- [20] Yang Y.B., Yau J.D., Hsu L.C.: *Vibration of simple beam due to trains moving at high speed*. Engineering Structures, 19, 11, 1997, 936-944.
- [21] Szafranski M.: *Vibration of the bridge under moving singular loads – theoretical formulation and numerical solution*. Journal of Applied Mathematics and Computational Mechanics, 15, 1, 2016, 169-180.
- [22] Fryba L.: *A Rough assessment of railway bridges for high-speed trains*. Engineering Structures, 23, 5, 2001, 548-556.
- [23] Li J., Su M.: *The resonant vibration for a simply supported girder bridge under high-speed trains*. Journal of Sounds and Vibration, 224, 5, 1999, 897-915.

- [24] Gou H., Zhou W., Yang Ch., Yi B., Pu Q.: *Dynamic response of a long-span concrete-filled steel tube tie arch bridge and the riding comfort of monorial trains*. Applied Sciences, 8, 4, 2018, 1-22.
- [25] Podworna M.: *Dynamic response of steel-concrete composite bridges loaded by high-speed train*. Structural Engineering and Mechanics, 62, 2, 2017, 179-196.
- [26] Zobel H., Zbiciak A., Oleszek R., Michalczyk R., Mossakowski P.: *Numerical identification of the dynamic characteristics of a steel-concrete railway bridge*. Roads and Bridges – Drogi i Mosty, 13, 3, 2014, 189-215, DOI: 10.7409/rabdim.014.018.
- [27] Kłasztorny M.: *Analiza dynamiczna belkowych mostów zespolonych na CMK w warunkach zwiększonych prędkości pociągów (160-250) km/h*. Roads and Bridges – Drogi i Mosty, 2, 3, 2003, 73-93.
- [28] Newmark N.M.: *A method of computation for structural dynamics*. J Eng Mech Div 1959;85(3):67-94.
- [29] *Sprawozdanie z wykonania próbnych obciążeń dynamicznych obiektów inżynierskich na szlaku Szeli – Idzikowice linii nr 4 CMK*, Wiadukt w km 26,571/26,578, Warszawa, listopad 2012 r.
- [30] Normy PN-EN 1991-2:2007 Eurokod 1: *Oddziaływania na konstrukcje – Część 2: Obciążenia ruchome mostów*.
- [31] PN-82/S-10052 *Obiekty mostowe. Konstrukcje stalowe. Projektowanie*.
- [32] PN-89/S-10052 *Obiekty mostowe. Konstrukcje stalowe. Wymagania i badania*.
- [33] PN-EN 1992-2:2005 Eurokod 2: *Projektowanie konstrukcji z betonu – Część 2: Mosty betonowe – Projektowanie i szczegółowe zasady*.
- [34] PN-EN 1993-2:2006 Eurokod 2: *Projektowanie konstrukcji stalowych – Część 2: Mosty stalowe – Projektowanie i szczegółowe zasady*.
- [35] PN-EN 1994-2:2005 Eurokod 4: *Projektowanie konstrukcji zespolonych stalowo-betonowych – Część 2: Reguły ogólne i reguły dla mostów*.